the cell, whereas distal inhibition will make the cell less responsive but still able to fire at its highest uninhibited rate when stimulated more strongly. In essence, the dynamic range of the cell is reduced by proximal but unaffected by distal inhibition.

Thus, when computational requirements dictate that inhibition be absolute, we would expect proximally placed inhibitory synapses. In contrast, when it is necessary that inhibition be overridden by sufficient excitation or when it is necessary to decrease the responsiveness of a neuron without reducing its dynamic range, distal inhibition should be used. Many computations performed by neural circuits must require inhibition that is relative (*13*). We suggest that this may be a major reason for the ubiquity of distal inhibition in higher nervous systems.


REFERENCES AND NOTES

1. R. Llinas and C. Nicholson, *J. Neurophysiol.* **34**, 532 (1971); Y. Fujita, *Brain Res.* **175**, 59 (1979); K. Mori *et al.*, *J. Neurosci.* **9**, 2291 (1984).
2. W. Rall, in *Neural Theory and Modeling*, R. F. Reiss, Ed. (Stanford Univ. Press, Palo Alto, CA, 1964), pp. 73–97; R. Llinas, in *Advances in Neurology*, G. W. Kreutzberg, Ed. (Raven, New York, 1975), vol. 12, pp. 1–13; J. J. B. Jack, D. Noble, R. W. Tsien, *Electric Current Flow in Excitable Cells* (Oxford Univ. Press, New York, 1975), pp. 197–213; G. M. Shepherd and C. Koch, in *The Synaptic Organization of the Brain*, G. M. Shepherd, Ed. (Oxford Univ. Press, New York, ed. 3, 1990), pp. 439–473.
3. A. Roberts, *J. Exp. Biol.* **48**, 545 (1968).
4. F. B. Krasne and J. J. Wine, *ibid.* **63**, 433 (1975); F. B. Krasne and S. C. Lee, *J. Neurosci.* **8**, 3703 (1988).
5. J. J. Wine and F. B. Krasne, *J. Exp. Biol.* **56**, 1 (1972).
6. Crayfish (*Procambarus clarkii*) were anesthetized by cooling, then their hemolymph was replaced with cold, aerated Ringer solution [A. van Harreveld, *Proc. Soc. Exp. Biol. Med.* **34**, 428 (1936)] to prevent clotting.
7. A connective between two abdominal ganglia was isolated from the circulating Ringer solution by a chamber in which Ringer and an isotonic sucrose solution could be exchanged.
8. Shocking the second ganglionic root recruits mechanosensory fibers that excite LG both mono- and disynaptically via a pool of interneurons [F. B. Krasne, *J. Exp. Biol.* **50**, 29 (1969)]. Recurrent inhibition reduced the monosynaptic component of root-evoked EPSPs by the same amount as the EPSP in Fig. 2, B1, but reduced the disynaptic component more because of additional inhibition at the first synapse of the circuit.
9. Data from (*3*) provide a value of 0.788 for the relative reductions of $\Delta V$ and EPSPs.
10. Tonic inhibition is largely if not wholly due to postsynaptic inhibition: it substantially shunts current passed between the bilateral LGs via their distal, electrical, and commissural junction (E. T. Vu and F. B. Krasne, in preparation).
11. This test was impractical for recurrent inhibition because of the additional inhibition at the first synapse of the LG circuit, which prevented experimental generation of strong input to LG during recurrent inhibition.
12. C. A. Terzuolo, R. L. Purple, E. Bayly, E. Handelman, in *Structure and Function of Inhibitory Neuronal Mechanisms*, C. von Euler, S. Skoglund, U. Soderberg, Eds. (Pergamon, New York, 1968), pp. 261–289.
13. For example, lateral inhibition in sensory systems [C. Koch, T. Poggio, V. Torre, *Trends Neurosci.* **9**, 204 (1986)], or the input function rules for units in distributed networks [J. L. McClelland and D. E. Rumelhart, Eds., *Parallel Distributed Processing* (MIT Press, Cambridge, MA, 1986)].
14. The equivalent circuit in Fig. 1, which is conventional for representing excitatory chemical transmission, is also appropriate for the LG excitation via rectifying electrical junctions [D. H. Edwards, W. J. Heitler, E. M. Liese, R. A. Fricke, *J. Neurosci.* **11**, 2117 (1991)]. In Fig. 1, $E_e$ represents the amplitude of the presynaptic spike and $G_e$ the lumped conductances of all forward biased junctions. Although steady-state predictions are presented here, extensive modeling with a realistic compartmental model of LG and synaptic potentials that mimic observed ones give qualitatively similar predictions (E. T. Vu and F. B. Krasne, in preparation).


15. We thank M. Konishi and C. Koch for discussion and T. Teshiba for technical assistance. Supported by a predoctoral NSF fellowship to E.T.V. and by National Institute of Neurological Diseases and Stroke grant NS-08108.

11 October 1991; accepted 14 January 1992


# The Size of Gating Charge in Wild-Type and Mutant *Shaker* Potassium Channels


NATHAN E. SCHOPPA, KEN MCCORMACK, MARK A. TANOUYE, FRED J. SIGWORTH*



**The high sensitivity of voltage-gated ion channels to changes in membrane potential implies that the process of channel opening is accompanied by large charge movements. Previous estimates of the total charge displacement, $q$, have been deduced from the voltage dependence of channel activation and have ranged from 4 to 8 elementary charges ($e_0$). A more direct measurement of $q$ in *Drosophila melanagaster Shaker* 29-4 potassium channels yields a $q$ value of 12.3 $e_0$. A similar $q$ value is obtained from mutated *Shaker* channels having reduced voltage sensitivity. These results can be explained by a model for channel activation in which the equilibria of voltage-dependent steps are altered in the mutant channels.**


HODGKIN AND HUXLEY (*1*) NOTED that the voltage sensitivity of sodium and potassium channels requires that charges must move in response to changes in membrane potential to open the channels. Recent structure-function studies of voltage-gated channels suggest that these voltage-sensing charges are the charged amino acid residues in the fourth putative transmembrane region called S4 (*2*). The best experimental support for this claim is that mutations that neutralize these charges decrease the voltage sensitivity of the channels (*3–5*). However, some mutations in the S4 region of *Shaker* $K^+$ channels that do not alter the number of charges on the amino acid side chains also decrease the voltage sensitivity of activation (*4, 6*). One explanation is that mutations that do not alter charge decrease the total charge displacement by reducing the distance charged moieties move within the membrane electric field. Alternatively, these mutations may not reduce the total charge displacement at all, but may change the way in which charge displacement is coupled to channel opening. To distinguish between these two alternatives for one of these mutations, we measured the total single-channel charge displacement, $q$.

We compared truncated wild-type (WT) *Shaker* 29-4 channels from *Drosophila* (*7*) with truncated mutated channels (V2) in which $Leu^{370}$, located near the end of the S4 region, was replaced with Val (Fig. 1A) (*6, 8*). *Shaker* channels normally show rapid inactivation; that is, they open only transiently during depolarization. We used truncated channels in which residues 2 to 29 were deleted to eliminate inactivation (*9*) and allow equilibrium measurements of channel opening and gating charge. Compared to WT channels, V2 channels showed a shift of ~+40 mV in their threshold of activation (Fig. 1, B and C), consistent with shifts in nontruncated channels having this mutation (*6, 10, 11*), and also had reduced voltage sensitivity of activation (*6*).

We first obtained estimates of the total single-channel charge displacement from the voltage dependence of the channel open probability ($p_o$). We refer to these estimates as $q_a$. Given specific assumptions (*12*), $p_o$ is proportional to $\exp(qV/kT)$, where $k$ is the Boltzmann constant and $T$ is the absolute temperature, at membrane potentials ($V$) where $p_o$ approaches zero. Measuring $p_o$ values between $10^{-3}$ and $10^{-2}$, Liman and co-workers (*5*) estimated $q_a$ to be ~7 $e_0$ for the rat brain (RCK1) $K^+$ channel. In similar measurements of $q_a$ for the WT and V2


N. E. Schoppa, K. McCormack, F. J. Sigworth, Department of Cellular and Molecular Physiology, Yale University School of Medicine, New Haven, CT 06510.
M. A. Tanouye, Department of Entomology, University of California, Berkeley, CA 94720.

*To whom correspondence should be addressed.

channels (Fig. 1D), we obtained values of 9.5 ± 1.2 $e_0$ and 5.5 ± 0.5 $e_0$, respectively (mean ± SD; $n = 4$ in each case). These $q_a$ values should be taken as lower bounds on the true charge displacement, in part because we do not know if our measurements were made at sufficiently low open probabilities.

Charge displacements in channels can be recorded directly as gating currents (*13, 14*), and Stühmer and co-workers (*15*) demonstrated that such currents can be recorded in large membrane patches from oocytes expressing exogenous $K^+$ channels. With charybdotoxin (CTx) in the pipette and $Cs^+$ in the bath solution to block ionic currents, we observed transient currents both at the beginning of a depolarizing pulse ("on" currents) and after its end ("off" currents) that were roughly 1/200 the size of corresponding ionic currents (Fig. 2A) (*16*). Consistent with other observed gating currents of the $K^+$ channel (*15, 17, 18*), the amplitude and decay rate of the "on" currents increased with increasing depolarization. Although the kinetics of the "off" currents for the V2 and WT channels were clearly different (*19*), the size and kinetics of the "on" currents for the two channels were remarkably similar (Fig. 2A) in view of the large difference between their voltage dependence of channel activation (Fig. 1, B and C).

The "on" gating currents were integrated to estimate the total charge $Q$ moved in the patch at various potentials, with $Q_{max}$ being the maximum value obtained at large positive voltages. The voltage dependence of $Q$ for WT and V2 channels differed (Fig. 2B); the WT charge movement saturated by −10 mV, but V2 charge movement continued to increase at potentials up to +40 mV, suggesting that the V2 mutation shifted the voltage dependence of a component of charge movement. However, differences in the effect of the V2 mutation on the voltage dependence of activation and overall charge movement allowed us to observe charge movement at voltages near 0 mV even when the ionic current was not blocked (Fig. 2C).

For direct estimation of the single channel charge displacement, $q$, we measured the number of channels ($N$) and $Q_{max}$ in the same membrane patch. $N$ was determined by fluctuation analysis (*20*) of the ionic currents (Fig. 3, A and B): the mean and variance of an ensemble of current records were computed and fitted to yield estimates of $N$ and the single channel current (*21*). To determine $Q_{max}$, we measured gating currents after the replacement of bath $K^+$ with tetraethylammonium ion ($TEA^+$) to block ionic currents (Fig. 3C). $TEA^+$ was used rather than CTx because it acts from the cytoplasmic side of the membrane and could be added easily (*22*). The $Q_{max}$ value in

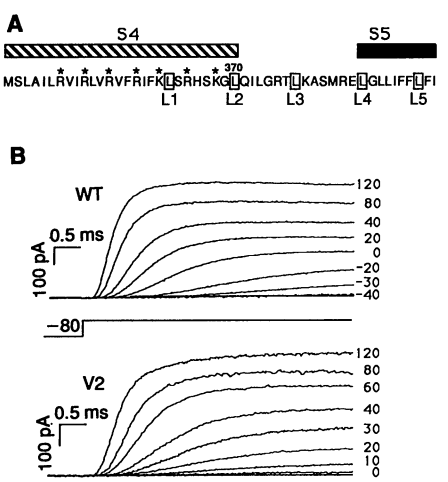


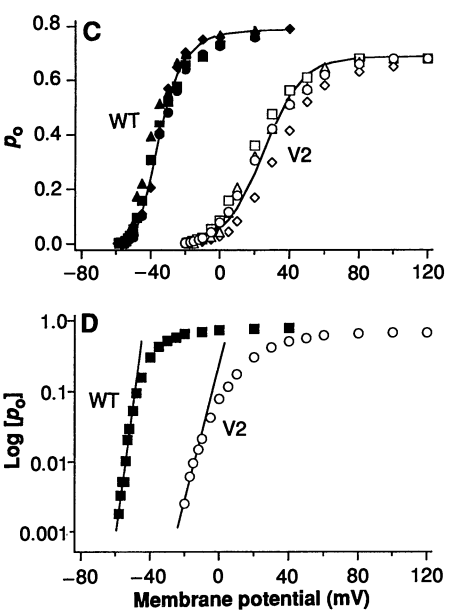


**Fig. 1.** Activation properties of WT and V2 channels in oocyte membrane patches. (**A**) Deduced amino acid sequence (*29*) of the leucine heptad-repeat region of *Shaker* 29-4 (*30*). Basic residues in S4 (asterisks) and leucine residues in the heptad repeat (boxed) are marked. (**B**) Outward WT and V2 $K^+$ currents measured in inside-out membrane patches evoked by steps from a holding potential of −80 mV to the potentials shown (in millivolts). Data were filtered at 10 kHz (Bessel response) and sampled at 50 kHz. The traces shown were P/4 subtracted and represent averages of 10 to 30 sweeps. Pipettes were filled with 140 mM *N*-methyl-D-glucamine aspartate, 1.8 mM $CaCl_2$, and 10 mM Hepes. The bath solution contained 140 mM potassium aspartate, 10 mM KCl, 1 mM EGTA, and 10 mM Hepes. (**C**) Voltage dependence of steady-state activation for WT and V2 channels. Data from four WT patches (closed symbols) and four V2 patches (open symbols) are shown. Superimposed curves are least-squares fits of our scheme for WT and V2 channel activation to the means of the points shown. For determining steady-state activation the current was measured at the end of 5- to 80-ms test pulses (for WT) and 8- to 30-ms test pulses (for V2). We obtained values for $p_o$ by first dividing the measured current by the instantaneous current-voltage (*I-V*) relation and then normalizing the result to the absolute peak $p_o$ determined by fluctuation analysis. (**D**) Activation curves from one experiment plotted semilogarithmically, with lines corresponding to slopes of 2.4 and 4.4 mV per e-fold change ($q_a$ = 10.6 and 5.6, respectively). Measurements of $q_a$ in this and other experiments were made at $0.0015 \leq p_o \leq 0.02$.

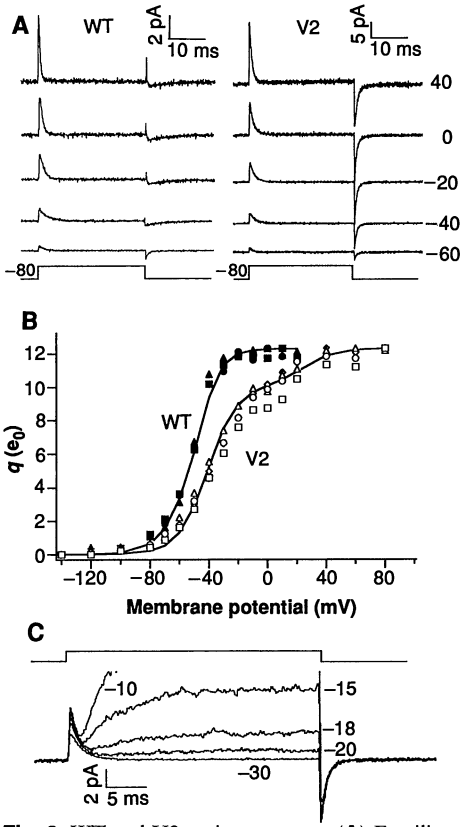


**Fig. 2.** WT and V2 gating currents. (**A**) Families of gating currents evoked by pulses from a holding potential of −80 mV to the potentials shown (in millivolts), measured with 2 μM of CTx-Lq1 toxin (*31*) [dissociation constant ($K_d$) ≈ 1.5 nM] in the *N*-methyl-D-glucamine aspartate pipette solution, and with $Cs^+$ replacing $K^+$ in the bath solution. Averages of 10 to 150 sweeps, filtered at 5 kHz, are shown. (**B**) Charge movement as a function of test potential. Plotted are three WT (closed symbols) and four V2 (open symbols) experiments. Superimposed curves are least-squares fits of our scheme for WT and V2 channels to the means of the plotted points. We obtained values of the charge movement in the patch, $Q$, by numerically integrating the "on" transients above a baseline current that was assumed to switch on with the rise time of the 5-kHz filter and that was calculated by averaging the current during the second half of the depolarizing pulses (*32*). The ordinate represents values generated by first normalizing the measured $Q$ values to the $Q_{max}$ value of the patch and then scaling according to the estimated maximum charge movement per channel $q$ = 12.3 $e_0$. (**C**) Gating currents that precede the activation of ionic currents in V2 channels observed in the absence of channel blockers at membrane potentials between −30 and −10 mV.

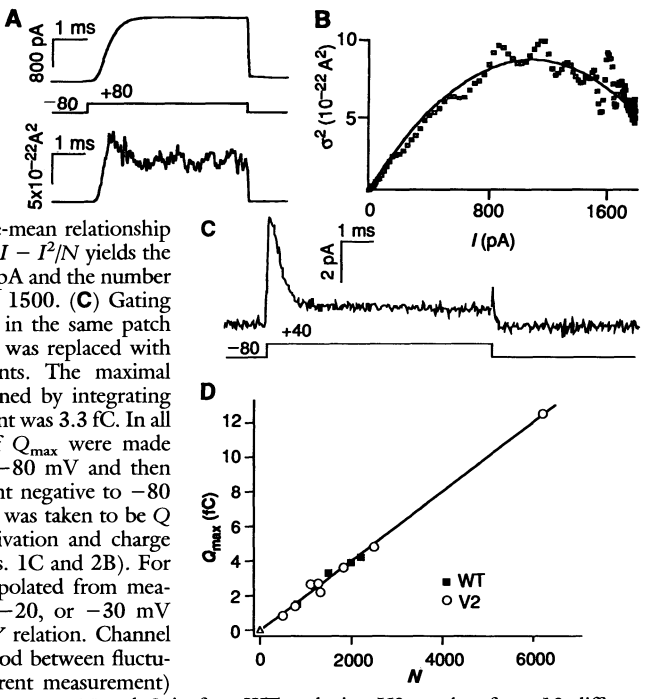


**Fig. 3.** Estimation of $q$ in a membrane patch that contained WT channels. (**A**) Mean current, $I$, from 76 depolarizations to +80 mV (top) and the corresponding time course of the variance, $\sigma^2$ (bottom). Data were filtered at 15 kHz and sampled at 100 kHz. (**B**) The variance-mean relationship fitted according to (*20*) $\sigma^2 = iI - I^2/N$ yields the single channel current $i$ = 1.5 pA and the number of channels in the patch $N \approx 1500$. (**C**) Gating current at +40 mV recorded in the same patch after $K^+$ in the bath solution was replaced with $TEA^+$ to block ionic currents. The maximal charge movement $Q_{max}$ obtained by integrating the "on" gating current transient was 3.3 fC. In all experiments measurements of $Q_{max}$ were made from a holding potential of −80 mV and then corrected for charge movement negative to −80 mV (Fig. 2B). For WT, $Q_{max}$ was taken to be $Q$ at +40 mV, where both activation and charge movement had saturated (Figs. 1C and 2B). For V2 channels, $Q_{max}$ was extrapolated from measurements of $Q$ at +40, 0, −20, or −30 mV according to the average $Q$-$V$ relation. Channel rundown in ~5 min (the period between fluctuation analysis and gating current measurement) was negligible. (**D**) Relation between $N$ and $Q$ in four WT and nine V2 patches from 12 different oocytes having expression levels that spanned an order of magnitude. The triangle near the origin represents an additional V2 patch that contained a single channel.

different patches was proportional to $N$ (Fig. 3D) and was unmeasurable in a patch where $N$ was equal to 1, implying that the charge movement measured arose only from exogenous *Shaker* channels. From ratios of $Q_{max}$ to $N$ we obtained values for $q$ of 12.4 ± 1.2 $e_0$ ($n$ = 3) and 12.2 ± 2.1 $e_0$ ($n$ = 5) for WT and V2 channels, respectively.

The estimate of 12.4 $e_0$ for the single channel charge displacement of WT channels is higher than previous values (*5, 13, 14, 23*). Our measurement may include charge movement not directly involved in activation—for example, charge movement associated with conformational changes that occur after the channel is already open. Our value is, however, not much larger than our lowest estimate for $q$ of WT channels obtained from the voltage dependence of activation ($q_a$ = 9.5 $e_0$). [A similar value, $q$ = 9.3, was also obtained in a study of activation kinetics of *Shaker* channels (*24*).] In this context, the WT channels appear to be quite efficient. These results place an upper bound of ~3 $e_0$ on the size of the charge movement not directly involved in channel activation.

The estimate of 12.2 $e_0$ for single channel charge displacement in V2 channels is remarkably similar to that for WT channels. The large difference between $q$ and the estimate from the voltage dependence of activation ($q_a$ = 5.5 $e_0$) for V2 channels raises the question of how these channels can have almost the same amount of total charge movement as WT channels but display a lower voltage sensitivity. One possibility is that some of the charge movement in V2 is completely uncoupled from the channel-opening process.

Another explanation can be found if we do not assume that the channel-gating process involves equivalent voltage-dependent transitions. The effect of the V2 mutation can then be explained through a shift in the equilibrium of one or more of these transitions. For example, a scheme derived from activation models for the *Shaker* channel (*24*) and for the RCK1 channel (*25*),

$$C_0 \underset{4K_0}{\rightleftharpoons} C_1 \underset{\frac{3}{2}K_0}{\rightleftharpoons} C_2 \underset{\frac{2}{3}K_0}{\rightleftharpoons} C_3 \underset{\frac{1}{4}K_0}{\rightleftharpoons} C_4 \underset{K_4}{\rightleftharpoons} C_5 \underset{K_5}{\rightleftharpoons} O$$

can account for the properties of both WT and V2 channels described here. In this scheme, four independent voltage-dependent transitions between closed states ($C_0$ to $C_4$) with a microscopic equilibrium constant $K_0$ (these transitions are shown as sequential but with appropriate statistical factors) are followed by one additional voltage-dependent step (between $C_4$ and $C_5$) with equilibrium $K_4$ and a final voltage-independent step leading to the channel opening (O) with equilibrium $K_5$. The equilibrium constants are the ratio of forward to backward rate constants. $K_0$ and $K_4$ are associated with charge movements $q_0$ and $q_4$, and are therefore voltage-dependent according to $K_i = \exp[(V - V_i)q_i/kT]$.

Simultaneous fits of this scheme were made to the voltage dependence of $p_o$ and $Q$, subject in each case to the constraint that the total charge movement, $4q_0 + q_4$, is equal to 12.3 $e_0$. Values of 2.5 and 2.3 $e_0$ for $q_0$ and $q_4$, respectively, provided acceptable fits to both the WT and V2 data (Figs. 1C and 2B). The differences between WT and V2 were accounted for by different midpoint voltages, $V_i$. For the WT data $V_0$ and $V_4$ were −53 and −25 mV, respectively, and $K_5$ was 3.7; for V2 the fitted values were −41 and +38 mV, and $K_5$ was 2.2.

Although our scheme does not completely describe *Shaker* channel gating (*26*), it does reflect several properties of these channels. First, the similarity in the size and time course of WT and V2 "on" gating currents (Fig. 2A) is reflected in our model's similar values for the midpoint voltage ($V_0$) of the first four transitions, where 10 of the 12.3 $e_0$ of charge movement occurs. Second, the shallower voltage dependence of $Q$ in V2 channels (Fig. 2B) is explained by the disparate midpoint voltages $V_0$ and $V_4$, yielding a broad curve with partially resolved components. The fact that V2 channels displayed a shifted and reduced voltage dependence of opening compared to WT channels is likewise explained by the shifted $V_4$: channels become trapped in state $C_4$ when $V$ is between −40 and 0 mV, and above 0 mV the voltage dependence of opening primarily reflects the voltage dependence of the $C_4$ to $C_5$ transition.

The effect of the V2 mutation can be explained by the existence of several components of gating charge movement, one of which has its equilibrium shifted by the mutation. In the context of our scheme, these components are associated with distinct early and late transitions that accompany channel opening. In $Na^+$ channels, the effect of $D_2O$ substitution (*14, 27*) and high pressure (*28*) is to slow channel activation with little effect on gating-current kinetics, consistent with the idea of early voltage-dependent and late voltage-independent activation transitions. Single channel (*24, 25*) and gating-current (*15, 18*) recordings from $K^+$ channels also suggest such a mechanism. The effects of the V2 mutation, however, suggest that there is a small but distinguishable charge movement associated with a late transition in channel activation.

The $Leu^{370}$ residue is close to the S4 charges thought to be the voltage-sensing charges leading to channel opening, and it is possible that the late as well as the early transitions might involve the movement of S4 charges. However, our results call into question an assumption in experiments that support the S4 hypothesis. For the V2 channel a large discrepancy exists between the amount of gating charge estimated from the voltage dependence of activation and that estimated from our direct measurement

(5.5 $e_0$ versus 12.3 $e_0$). The fact that $q$ for the V2 channel, as measured through voltage sensitivity of activation, is underestimated shows that estimates of $q$ obtained in this way must be interpreted carefully.


REFERENCES AND NOTES

1. A. L. Hodgkin and A. F. Huxley, *J. Physiol. (London)* **117**, 500 (1952).
2. M. Noda *et al.*, *Nature* **312**, 121 (1984).
3. W. Stühmer *et al.*, *ibid.* **339**, 597 (1989).
4. D. M. Papazian, L. C. Timpe, Y. N. Jan, L. Y. Jan, *ibid.* **349**, 305 (1991).
5. E. R. Liman, P. Hess, F. Weaver, G. Koren, *ibid.* **353**, 752 (1991).
6. K. McCormack *et al.*, *Proc. Natl. Acad. Sci. U.S.A.* **88**, 2931 (1991).
7. L. E. Iverson and B. Rudy, *J. Neurosci.* **10**, 2903 (1990).
8. Construction of inactivating WT and V2 *Shaker* 29-4 cDNA and in vitro synthesis of mRNA is described (*6*, 7). WT and V2 channels were made noninactivating by replacement of the Sac I–Nar I fragment from the *Shaker* 29-4 Bluescript (Stratagene) construct with complementary oligonucleotides that deleted amino acid residues 2 to 29. The constructs were sequenced to ensure that only the appropriate changes were introduced. *Xenopus laevis* oocytes were injected with WT or V2 mRNA (~3 ng) and patch-clamped 4 to 21 days later. Conventional oocyte macropatch techniques were used (*15*) with pipettes having a 3- to 10-μm diameter (0.5- to 2.0-megohm resistance) pulled from Kimax capillaries. Recordings were made from inside-out membrane patches at 21° to 23°C with an EPC-9 patch clamp (Heka Electronic, Lambrecht, Germany).
9. T. Hoshi, W. N. Zagotta, R. W. Aldrich, *Science* **250**, 533 (1990).
10. K. McCormack, J. W. Lin, L. E. Iverson, B. Rudy, *Biochem. Biophys. Res. Commun.* **171**, 1361 (1990).
11. G. A. Lopez *et al.*, *Neuron* 7, 327 (1991).
12. W. Almers, *Rev. Physiol. Biochem. Pharmacol.* **82**, 96 (1978).
13. C. M. Armstrong and F. Bezanilla, *Nature* **242**, 459 (1973); R. D. Keynes and E. Rojas, *J. Physiol. (London)* **239**, 393 (1974); W. Nonner, E. Rojas, R. Stämpfli, *Pfluegers Arch.* **375**, 75 (1975).
14. H. Meves, *J. Physiol. (London)* **243**, 847 (1974).
15. W. Stühmer, F. Conti, M. Stocker, O. Pongs, S. H. Heinemann, *Pfluegers Arch.* **418**, 423 (1991).
16. For the subtraction of linear leakage currents in the gating-current recordings, alternating positive and negative 20-mV pulses were applied from −120 mV and the responses were subtracted and scaled appropriately to the test pulse. Artifacts resulting from charge movement during the −120- to −100-mV leak subtraction pulses were estimated and corrected (*15*). However, we were unable to correct for charge movement during the −120- to −140-mV pulses, which might have slightly distorted the initial phases of the gating currents. The "on" gating currents did not show a rising phase, as was reported in gating currents from another truncated, noninactivating *Shaker* channel (*18*). The origin of this discrepancy is unclear although it may involve differences in the recording technique (whole-oocyte versus patch recordings) or differences in the *Shaker* constructs used.
17. F. Bezanilla, M. M. White, R. E. Taylor, *Nature* **296**, 657 (1982); M. W. White and F. Bezanilla, *J. Gen. Physiol.* **85**, 539 (1985); S. Spires and T. Begenisich, *ibid.* **93**, 263 (1989).
18. F. Bezanilla, E. Perozo, D. M. Papazian, E. Stefani, *Science* **254**, 679 (1991).
19. The difference in the decay rates of the V2 and WT "off" gating currents is probably related to the fact that deactivation in V2 channels occurs much more rapidly than in WT channels. The time constants of decay for "off" gating currents and ionic tail currents following a large depolarization were both ~5 ms for the WT channel and ~0.75 and 0.20 ms, respectively, for the V2 channel.
20. F. J. Sigworth, *J. Physiol. (London)* **307**, 97 (1980).
21. As a check for the reliability of the fluctuation analysis results, estimates for single channel current ($i$) and $p_o$ (1.5 ± 0.2 pA and 0.79 ± 0.08 for WT at +80 mV, $n$ = 8; 1.3 ± 0.2 pA and 0.68 ± 0.08 for V2 at +160 mV, $n$ = 9) were compared with and found to be very close to those obtained from parallel single channel recordings (1.7 pA, 0.80, 1.5 pA, and 0.55, respectively). However, the V2 channel displays variable kinetics and multiple conductance levels, with $i$ at +160 mV most commonly ~1.5 or ~3 pA. To check the validity of the fluctuation analysis results for the V2 channels more directly, we analyzed recordings from patches where there was a known number of V2 channels. In three patches containing one, one, and three channels, fluctuation analysis of the ensembles (280, 450, and 149 records, respectively) yielded $N$ values of 1.0, 1.5, and 2.8. These results and theoretical considerations suggest that systematic errors in the fluctuation analysis, if present, would tend toward overestimation of $N$ and thus underestimation of $q$ for the V2 channel.
22. $TEA^+$ might be expected to interfere with the "on" charge movement, as (unlike CTx) it appeared to abolish the "off" charge movement (Fig. 3C) at large depolarizations, as reported previously for truncated *Shaker* H4 (*18*). However, $TEA^+$ added to the bath did not change the time course and amplitude of "on" currents in other patches that contained WT or V2 channels already blocked by CTx. Moreover, measurements of V2 gating currents made without ionic currents blocked yielded similar estimates of $q$ (12.6 ± 0.3 $e_0$, $n$ = 3), as did two additional experiments where tetramethylammonium ion, which does not block the "off" currents, was used in the bath solution instead of $TEA^+$ (12.2 and 11.2 $e_0$ for WT and V2, respectively).
23. L. C. Timpe *et al.*, *Neuron* **1**, 659 (1988); L. E. Iverson *et al.*, *Proc. Natl. Acad. Sci. U.S.A.* **85**, 5723 (1988).
24. W. N. Zagotta and R. W. Aldrich, *J. Gen. Physiol.* **95**, 29 (1990).
25. G. Koren *et al.*, *Neuron* **2**, 39 (1990).
26. For both WT and V2 channels, a long delay precedes the rise of ionic currents following a step depolarization (Fig. 1B). To fit the time course of the currents, at least 12 closed states were required for a linear scheme to account for the delay.
27. C. L. Schauf and M. A. Chuman, in *Ion Channels in Neural Membranes*, J. M. Ritchie, D. R. Keynes, L. Bolis, Eds. (Liss, New York, 1986), p. 3.
28. F. Conti, I. Inoue, F. Kukita, W. Stühmer, *Eur. Biophys. J.* **11**, 137 (1984).
29. Abbreviations for the amino acid residues are: A, Ala; E, Glu; F, Phe; G, Gly; H, His; I, Ile; K, Lys; L, Leu; M, Met; Q, Gln; R, Arg; S, Ser; T, Thr; and V, Val.
30. A. Kamb *et al.*, *Neuron* **1**, 421 (1988).
31. K. Lucchesi, A. Ravindran, H. Young, E. Moczydlowski, *J. Membr. Biol.* **109**, 269 (1989).
32. Alternative $Q$ estimates that would be insensitive to the uncorrected charge movement between −120 and −140 mV were obtained by fitting the "on" gating currents to one or two exponentials plus a constant term and taking $Q$ to be the integral of the exponential function. The resulting values were within ~10% of those obtained by numerical integration. Estimates of $q$ obtained by fitting the "on" gating currents were an average of 8% larger than those obtained by numerically integrating the currents.


33. We thank L. Iverson for making some of the cRNA; T. McCormack for sequence verification of noninactivating deletion constructs; L. Lin for oocyte preparation; E. Moczydlowski for CTx; S. H. Heinemann for helpful discussions; and W. K. Chandler and T. Woolf for comments on the manuscript. Supported by NIH grants to F.J.S., M.A.T., and L. Iverson.

16 October 1991; accepted 14 January 1992


# Tumor Necrosis Factor–α Activates the Sphingomyelin Signal Transduction Pathway in a Cell-Free System


KENNETH A. DRESSLER, SHALINI MATHIAS, RICHARD N. KOLESNICK*



**The mechanism of tumor necrosis factor (TNF)–α signaling is unknown. TNF-α signaling may involve sphingomyelin hydrolysis to ceramide by a sphingomyelinase and stimulation of a ceramide-activated protein kinase. In a cell-free system, TNF-α induced a rapid reduction in membrane sphingomyelin content and a quantitative elevation in ceramide concentrations. Ceramide-activated protein kinase activity also increased. Kinase activation was mimicked by addition of sphingomyelinase but not by phospholipases $A_2$, C, or D. Reconstitution of this cascade in a cell-free system demonstrates tight coupling to the receptor, suggesting this is a signal transduction pathway for TNF-α.**


SPHINGOMYELIN CAN BE METABOlized to generate molecules that have various functions within the cell (*1–5, 6*). Ceramide, which is generated by sphingomyelinase action, can be deacylated to sphingoid bases (*1, 2*), which are potential inhibitors of protein kinase C (*3*) or phosphorylated to ceramide 1-phosphate (*4*) by a ceramide kinase (*5*). Ceramide appears to have bioeffector properties (*7, 8*). Cell-permeable ceramide analogs stimulate monocytic differentiation of human leukemia (HL-60) cells (7) and the phosphorylation of the epidermal growth factor receptor (EGFR) at $Thr^{669}$ in A431 human epidermoid carcinoma cells (*8*). TNF-α activates a neutral sphingomyelinase to generate ceramide in HL-60 cells, and it was postulated that this initiated TNF-α action (*9*). We defined a ceramide-activated protein kinase with a synthetic peptide derived from the amino acid sequence surrounding $Thr^{669}$ of the EGFR (residues 663 to 681) (*10*). Kinase activity was membrane-associated, $Mg^{2+}$-dependent, and activated by natural or synthetic ceramide in a concentration- and time-dependent manner. This ceramide-


Laboratory of Signal Transduction, Sloan-Kettering Institute, Memorial Sloan-Kettering Cancer Center, New York, NY 10021.

*To whom correspondence should be addressed.